

Research

Identification of critical biomarkers and immune landscape patterns in glioma based on multi-database

Hanzhang Yuan¹ · Jingsheng Cheng² · Jun Xia² · Zeng Yang² · Lixin Xu²

Received: 11 July 2024 / Accepted: 28 November 2024

Published online: 13 January 2025

© The Author(s) 2025 [OPEN](#)

Abstract

Purpose Glioma is the most prevalent tumor of the central nervous system. The poor clinical outcomes and limited therapeutic efficacy underscore the urgent need for early diagnosis and an optimized prognostic approach for glioma. Therefore, the aim of this study was to identify sensitive biomarkers for glioma.

Patients and methods Differentially expressed genes (DEGs) of glioma were downloaded from The Cancer Genome Atlas (TCGA) and Gene Expression Omnibus (GEO) databases. The potential biomarkers were identified using weighted gene co-expression network analysis (WGCNA) and least absolute shrinkage and selection operator (LASSO) regression. The prognostic ability of the potential biomarkers was evaluated by Cox regression and survival curve. CellMiner was used to access the correlation between the expression of potential biomarkers and anticancer drug sensitivity. We then explored the association of potential biomarkers and tumor immune infiltration by single-sample GSEA (ssGSEA) and CIBERSORT. Immune staining in glioma patient samples and cell experiments of potential biomarkers further verified their expression and function.

Results Ultimately, we identified three potential biomarkers: SLC8A2, ATP2B3, and SRCIN1. These 3 genes were found significantly correlated with clinicopathological features (age, WHO grade, IDH mutation status, 1p19q codeletion status). Furthermore, the overall survival (OS), disease-specific survival (DSS), and progression-free survival (PFS) were found to be positively correlated with high expression of these 3 potential biomarkers. Besides, there was a substantial relationship between the sensitivity of anticancer drugs and these biomarkers expression. More importantly, the negative association between the 3 genes with most tumor immune cells was also established. Moreover, the decreased expression of the biomarkers was also verified in glioma patient samples. Finally, we confirmed that these 3 genes might promote glioma proliferation and migration in vitro.

Conclusion SLC8A2, ATP2B3, and SRCIN1 were identified as underlying biomarkers for glioma associated with prognosis assessments and personal immunotherapy.

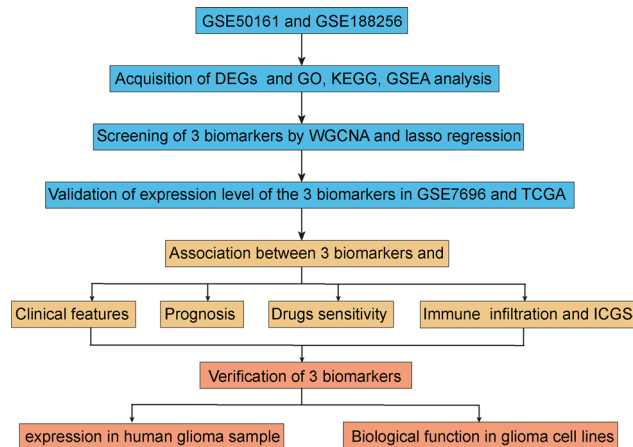
Supplementary Information The online version contains supplementary material available at <https://doi.org/10.1007/s12672-024-01653-2>.

Hanzhang Yuan and Jingsheng Cheng contributed equally.

✉ Lixin Xu, xlxmd2060@hotmail.com | ¹Department of Neurosurgery, Yueyang Central Hospital, Yueyang 414020, Hunan, China. ²Department of Neurosurgery, Changde Hospital, Xiangya School of Medicine, Central South University (The First People's Hospital of Changde City), Changde 415003, Hunan, China.



Graphical Abstract



Keywords Glioma · Biomarker · Hub genes · Prognosis · Anticancer agents · Immune infiltration

Abbreviations

TCGA	The Cancer Genome Atlas
GEO	Gene Expression Omnibus
LASSO	Least absolute shrinkage and selection operator
OS	Overall survival
DSS	Disease-specific survival
PFS	Progression-free survival
ssGSEA	Single-sample GSEA
CNS	Central nervous system
GBM	Glioblastoma
WHO	World Health Organization
NCCN	National comprehensive cancer network
IDH	Isocitrate dehydrogenase
MGMT	O6-methylguanine-DNA methyltransferase
EGFR	Epidermal growth factor receptor
DEGs	Differentially expressed genes
FDR	False discovery rate
GSEA	The gene set enrichment analysis
WGCNA	Weighted gene co-expression network analysis
WT	Wild type
Mut	Mutant type
TME	Tumor microenvironment
NK cells	Natural killer cells
Ths	Helper T cells
CTLs	T lymphocytes
T reg	Regulatory T

1 Introduction

Glioma is the most prevalent primary brain tumor, with significant implications for the central nervous system (CNS) [1, 2], and glioblastoma (GBM) is recognized as the most aggressive form of malignant brain tumor [3]. The standard therapeutic approach for glioma includes a combination of chemotherapy, radiation therapy, and surgical intervention [4]. However, the vast majority of patients with diffuse tumors continue to experience locoregional failure after treatment, leading to persistent or recurrent disease, notably GBM [5, 6]. This has stimulated the advancement of histological diagnostics and molecular stratification with the goal of more precisely determining tumor volume. Consequently, robust biomarkers are essential for the early recognition and personalized treatment that may enhance the prognosis of glioma.

The latest edition of the WHO and National Comprehensive Cancer Network (NCCN) guidelines emphasize the significance of molecular diagnostics in glioma [7]. The identification of multiple molecular features of gliomas have deepened our comprehension of the underlying pathogenesis of the disease [8–11]. Isocitrate dehydrogenase (IDH) is the primary biomarker that distinguishes different glioma entities. IDH mutations are considered pivotal early drivers and form the molecular basis for contemporary glioma classification [12]. Numerous clinical trials are underway for IDH-mutated glioma patients, yet a consensus on the optimal therapeutic approach remains elusive. O6-methylguanine-DNA methyltransferase (MGMT) methylation has been deemed another important prognostic biomarker. Elevated MGMT levels correlate with enhanced survival rates and increased sensitivity to alkylating agents [13]. While alkylating agents may enhance overall survival, their efficacy exhibits heterogeneity, and benefits are not uniformly observed across patient populations [14]. Furthermore, mutations in the epidermal growth factor receptor (EGFR) occur in about half of GBM patients, with 40% featuring gene amplifications linked to highly aggressive tumor phenotypes [15]. EGFR amplification or mutation is a prognostic indicator of unfavorable outcomes, despite reports suggesting ineffectiveness of EGFR-targeted therapies in certain GBM cases [16–18]. Despite extensive research on the aforementioned biomarkers, challenges persist, such as the need for broader validation of molecular markers and the development of efficacious biomarker-targeted therapies.

With the advent of high-throughput sequencing technologies, studies that integrate genome-wide data from large samples of different molecular platforms are progressively highlighting the advantages of discovering glioma subtypes. In the present work, we integrated gene expression profiles of tumor tissue samples from multiple datasets for analysis, powerful biomarkers were identified by a combination of weighted gene co-expression network analysis (WGCNA) and least absolute shrinkage and selection operator (LASSO) regression. The three biomarkers were found to be favorably correlated with patient prognosis and highly linked with clinicopathological characteristics (age, WHO grade, IDH mutation status, 1p19q codeletion status). There was an association between the three biomarkers and immune infiltration cells. Ultimately, histological immunofluorescence staining and cell experiments were applied to further validate to the expression and function of sensitive biomarkers for glioma.

2 Methods

2.1 Public databases collection and external validation cohort

The datasets containing normal and tumor samples were downloaded from the GEO database (www.ncbi.nlm.nih.gov/geo) and TCGA database (<https://cancergenome.nih.gov/>). The final downloaded dataset contains GSE50161, GSE7696 and GSE188256. The datasets downloaded from TCGA were used for prognostic analysis. Immunohistochemistry results of tissue sections from the HPA database (<https://www.proteinatlas.org/>) were used to compare protein expression between glioma and normal tissues. Furthermore, a total of 6 patients who had undergone glioma or brain trauma injury were enrolled in the external validation cohort, the detailed clinical information of included patients was presented in Supplementary Table 1.

2.2 Acquisition of differentially expressed genes

Data extraction and integration were performed by Perl software. The “limma” package of R software (version 4.1.3) was used to screen differentially expressed genes (DEGs) between tumor tissues and normal tissues by Bayes test with the filtering criteria of false discovery rate (FDR) < 0.05 and $\text{Log}_2|(\text{Fold change (FC)})| > 2$. We combined the two datasets to keep only the genes that were common to the dataset. Next, we used the Combat feature in the R package SVA to remove batch effects caused by the source of the dataset and preserve the biological differences between tumors and normal tissues. The heat map and volcano map were plotted with the R package “pheatmap” “ggplot2”.

2.3 Functional enrichment analysis of DEGs

The “clusterProfiler” “org.Hs.eg.db” “enrichplot” packages of R were combined to perform GO and KEGG enrichment analysis, and FDR < 0.05 was used as the screening criterion. The “ggplot2” and “circlize” packages were applied to draw histograms and enrichment maps. The Gene Set Enrichment Analysis (GSEA) enrichment analysis was performed by combining “limma”, “clusterProfiler”, “org.Hs.eg.db” and “enrichplot” packages to enrich the screened DEGs between the normal control group and tumor group. FDR < 0.05 was utilized as the screening criterion and GSEA enrichment plots were further developed.

2.4 WGCNA co-expression analysis of DEGs

WGCNA is a bioinformatics analysis method often used to efficiently explore the relationship between genes and phenotypes [19]. The genes contained in the training set were subjected to WGCNA co-expression analysis by the “limma” and “WGCNA” packages of R. Different gene modules were obtained, and the optimal module was selected and mapped using the “igraph” package. Relationships between phenotype and modules were to examine the significance of genes and clinical data. Candidate hub genes were selected from the gene set with the strongest connection among modules After that, the genes in the modules were intersected with the obtained DEGs, and a Venn diagram was drawn using the “venn” package.

2.5 Lasso regression of the intersecting genes to obtain disease biomarkers

Lasso regression is a method of variable screening by creating generalized linear regression [20]. The “glmnet” package was used to set the seed sequence to 111, and finally, the disease biomarkers were obtained by constructing the lasso regression model, and the lasso regression graph and the graph of cross-validation were demonstrated.

2.6 The effectiveness of patient’s reaction to chemotherapy

To analyze the correlation between risk score and medication sensitivity, researchers consulted the CellMiner database (<https://discover.nci.nih.gov/CellMiner>). CellMiner was used to access the mRNA profiles and IC50 values for drug sensitivity of NCI-60 human cancer cell lines. We then utilized the CellMiner database to make predictions about which medications could be effective at targeting the 3 biomarkers.

2.7 Immune infiltration analysis

The “reshape2”, “ggpubr”, “limma”, “GSEABase” and “GSVA” packages were used for ssGSEA immuno-infiltration analysis of normal controls and tumor samples [21], and “pheatmap” and “vioplot” packages were applied to create heat maps and violin maps. CIBERSORT was also used to evaluate the expression changes of a group of genes relative to all other genes in the sample [22]. The “limma”, “reshape2” and “tidyverse” packages of R were called to perform correlation analysis of immune cells and biomarkers by Spearman correlation analysis, and the correlation heat map was displayed by the “ggplot2” package.

2.8 Immunofluorescence

For immunofluorescence, the brain sections were rehydrated by different concentrations of alcohol and were retrieved through heating slides in citrate buffer using a pressure cooker. Concisely, tissue sections were incubated at 4 °C overnight with primary antibodies diluted in antibody diluent, at the following dilutions: anti-human ATP2B3(1:100, absin, China) and anti-human SRCIN1 (1:100, absin, China). The next day, the primary antibodies were detected by incubation of secondary antibodies (Proteintech, China) for 1 h at room temperature. The slides were counterstained with antifade mounting medium with DAPI (Beyotime, China). Olympus fluorescence microscope BX 51 (Japan) was used to capture images.

2.9 Cell culture and transfection

The U87 and U251 cell lines were purchased from American Type Culture Collection (ATCC). Cells were cultured in DMEM (Gibco, USA), supplemented with 10% fetal bovine serum (VivaCell, China), 1% L-glutamine (Procell, China), and 1% penicillin–streptomycin (Gibco, USA) at 37 °C with 5% CO₂ in a humidified cell incubator. Lipofectamine 3000 was used for transiently cell transfection according to the manufacturer's method.

2.10 Quantitative real time-PCR

Total RNA from cell was extracted using total RNA extraction kit (Vazyme, China) and the reversed transcribe cDNA was synthesized by transcription kit (Vazyme, China). Quantitative real time-PCR (qRT-PCR) was detected using SYBR Green Master Mix (Yeasen, China) according to the manufacturer's instructions in PCR instrument (Applied Biosystems, USA). The mRNA levels normalized to GAPDH were calculated by the $2^{-\Delta\Delta CT}$ method. The primer sequences were listed in Supplemental Table 2.

2.11 Apoptosis assay

10,000 cells per well were added to a 6-well plate for overnight, then the cells were transfected for 48 h. The cell apoptosis was evaluated using the Annexin V-FITC/PI apoptosis assay kit (Yeasen, China) according to the manufacturer's instructions. The cells were assessed by flow cytometer (Beckman, USA). A gating strategy is applied to exclude debris and cell aggregates from the analysis. Cells are categorized into four quadrants based on Annexin V and PI staining, representing viable, early apoptotic, late apoptotic, and necrotic populations. The percentage of cells in each category is calculated to quantify the apoptotic response.

2.12 Cell proliferation assay

Cells with a density of 4×10^4 /ml were cultured in a 96-well plate and incubated overnight before being transfected. The Cell Counting Kit 8 (CCK-8, Vazyme, China) was applied to measure cell proliferation, the absorbance at 450 nm was detected by an automated microplate reader (BioTek, USA).

2.13 Scratch assay

The scratch wound healing assay was utilized to evaluate the migratory ability of U87 and U251 cells. The wound was scraped with a 200 μ L pipette tip in a straight line. Then, the cells were incubated with DMEM media at 37 °C for 48 h. The cell images were captured at 0 h, 24 h and 48 h. The images captured at each time point are analyzed using ImageJ. The software is used to measure the wound distance between the wound edges at each time point. The percentage of wound closure is calculated as follows: Wound closure (%) = (Area at Time 0 – Area at Time X) / Area at Time 0 * 100%.

2.14 Migration assay

The Transwell chambers with 8 μ m pore size were used for migration experiments. 1×10^4 cells/well with serum-free media was seeded above the chambers, and medium containing 10% FBS was added in the lower chambers. After 24 h

incubation, the chambers were removed and fixed. Then migrated cells were stained by crystal violet and photographed by microscope (Olympus, Japan).

2.15 Western blot analysis

Cells were lysed RIPA buffer (Beyotime, China), and protein concentration was measure by BCA protein assay. Subsequently, the total protein separation was performed by 12% SDS-PAGE and transferred to a PVDF membrane. After 1 h block with 5% BSA, the membranes were successively incubated in primary and secondary antibodies and finally imaged in a chemiluminescence imager (Bio-Rad, USA). The Primary antibodies diluted in antibody diluent, at the following dilutions: anti-human SLC8A2 (1:500, ABclonal, China), anti-human ATP2B3 (1:1000, abcam, USA), anti-human SRCIN1 (1:100, Invitrogen, USA) and anti-human GAPDG (1:50,000, Proteintech, China). The intensity of the protein bands was quantified using ImageJ software and normalized to the corresponding loading control GAPDH to account for loading variations. The relative expression levels of the 3 proteins were quantified by gray value and expressed as a fold change relative to the GAPDH. Data were expressed as mean \pm SD and statistical significance was determined using a one-way ANOVA ($P < 0.05$).

2.16 Statistical analysis

All data are shown as mean \pm standard deviation (SD). P value from Student's t test to determine differences between two groups with normally distributed data and Mann Whitney test with other data. For multi groups, One-Way ANOVA was carried out for P value. $P < 0.05$ indicated statistical significance. * $P < 0.05$, ** $P < 0.01$, *** $P < 0.001$.

3 Results

3.1 Acquisition of DEGs between the control group and the glioma group

GSE50161 and GSE188256 downloaded from the GEO database were regarded as the training set. There were 168 samples, including 32 samples in the normal control group and 53 glioma samples. A total of 304 DEGs between glioma and normal samples were obtained after screening ($FDR < 0.05$, $\text{LogFC} > 2$). The heat map (Fig. 1A) and volcano map (Fig. 1B) demonstrated the different gene expression patterns in the control and glioma groups. Enrichment analysis was performed on the screened DEGs to better understand the biological processes and signal pathways linked with glioma. GO analysis revealed that these DEGs were mainly enriched in the modulation of chemical synaptic transmission, regulation

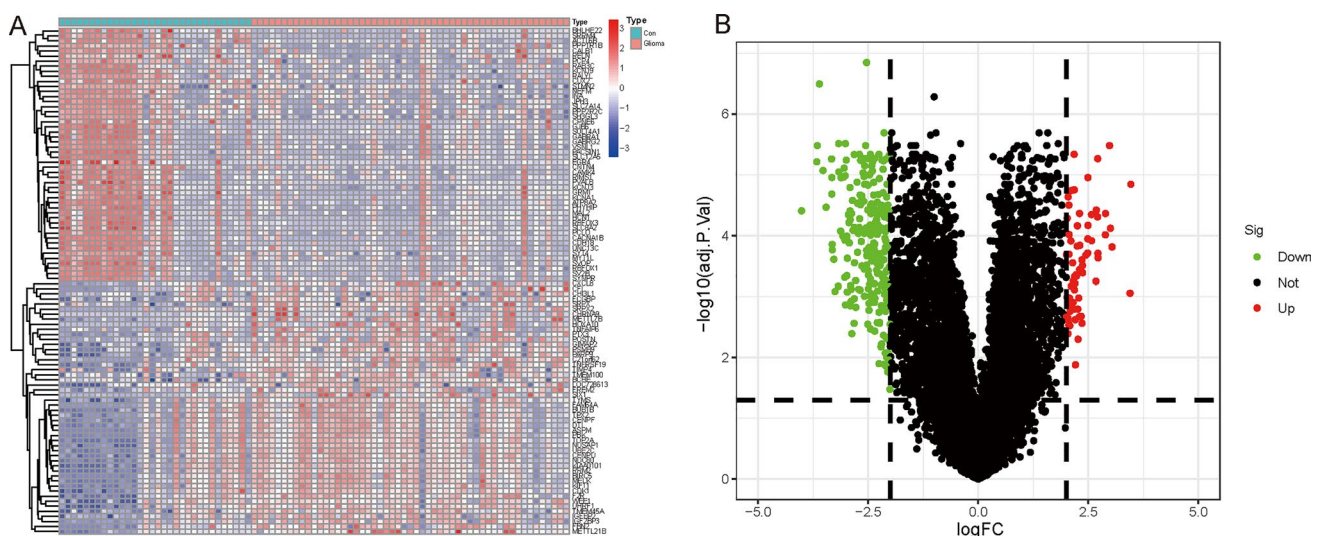


Fig. 1 Identification of DEGs between glioma and normal groups. **A** Heat map and **B** Volcanic map depicted dysregulated genes in glioma from the training set. DEGs, differentially expressed genes

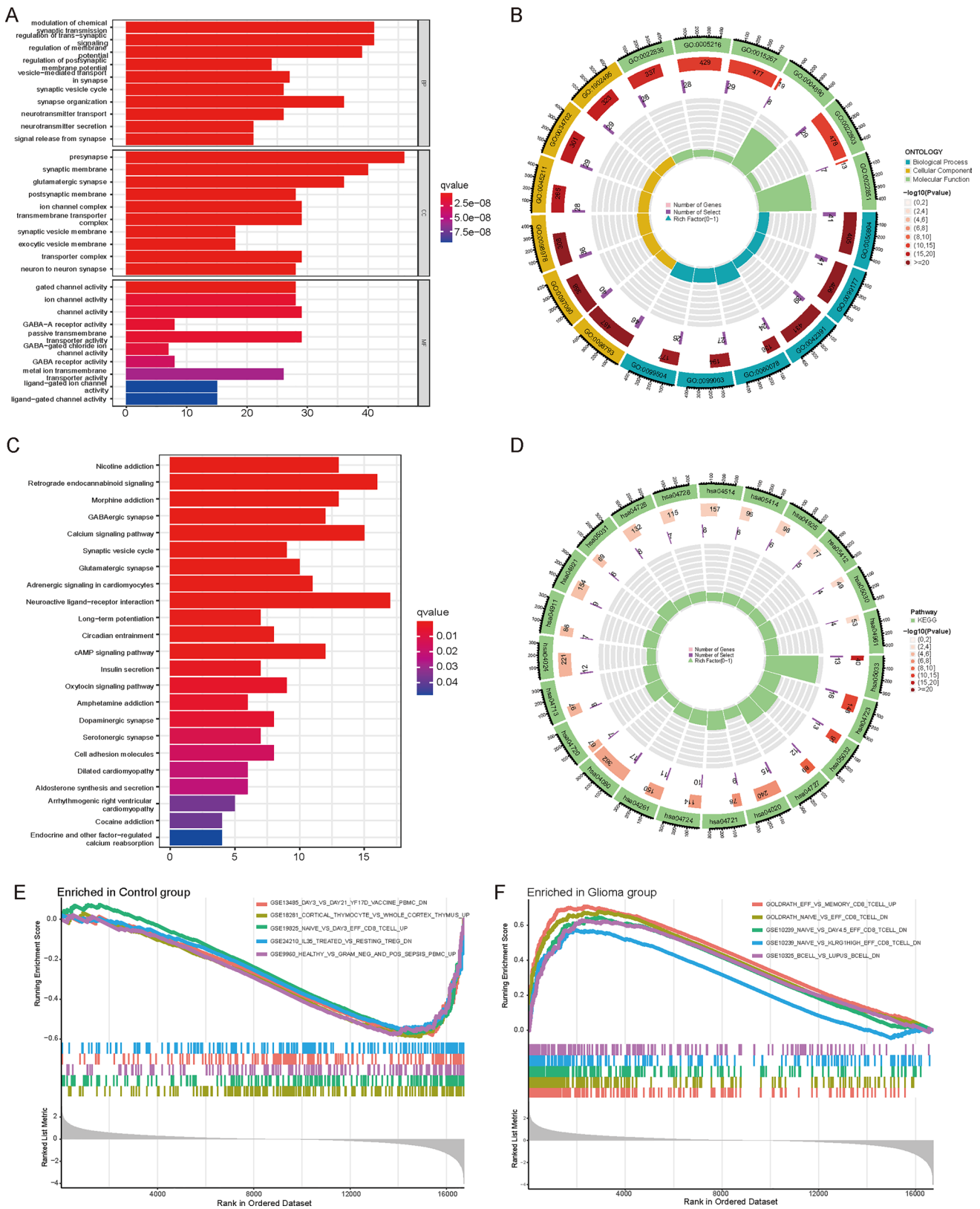


Fig. 2 Functional enrichment analysis of DEGs between glioma and normal groups. **A** Histogram and **B** Enrichment map illustrated GO annotation analysis of DEGs between the normal control group and the glioma group. **C** Histogram and **D** Enrichment map illustrated KEGG pathway analysis of DEGs between the normal control group and the glioma group. GSEA indicated the enrichment of various biological processes in the **E** control group and **F** glioma group

of trans-synaptic signaling, regulation of postsynaptic membrane potential, presynapse, and synaptic membrane (Fig. 2A and B). KEGG analysis uncovered that DEGs were mainly enriched in neuroactive ligand-receptor interaction, nicotine addiction, retrograde endocannabinoid signaling, morphine addiction, GABAergic synapses, calcium signaling pathways, and adrenergic signaling in cardiomyocytes pathways (Fig. 2C and D). Furthermore, GSEA analysis was performed on the normal control and glioma groups in the training set. In the control group, GSEA was mainly enriched in down-regulated YF17D vaccine, up-regulated thymic cortex, and up-regulated EFFCD8T cells. While tumor samples were mainly enriched in memory upregulated CD8T cells, downregulated EFFCD8T cells, and downregulated lupus cells (Fig. 2E and F).

3.2 Screening of biomarkers by WGCNA and lasso regression

WGCNA could be used to identify gene collection modules with similar expression patterns by calculating the expression relationships between DEGs. By resolving the linkage between gene collection modules and sample phenotypes, we then mapped the regulatory network between genes in the module and identified key regulatory genes. In this study, “WGCNA” in R was used to classify the DEGs into 10 modules with the best POWER value of 5, namely “MEpink”, “MEagenta”, “MEgreen”, “MEturquoise”, “MEblack”, “MEblue”, “MERed”, “MEbrown”, “MEpurple”, and “MEgrey” (Fig. 3A), and the “MEturquoise” module which had the strongest association with gene significance was selected for subsequent model construction and analysis (Fig. 3B). The correlation analysis illustrated a strong correlation between module membership and gene significance for glioma (Fig. 3C). Subsequently, the 20 candidate hub genes were selected from the intersection of genes in the “MEturquoise” module and DEGs (Fig. 3D). Eventually, we narrowed down the 20 candidate genes by the lasso regression approach to 3 genes, SLC8A2, ATP2B3, and SRCIN1, respectively. These 3 genes were considered to be the potential diagnostic biomarkers for glioma (Fig. 3E and F).

3.3 Validation of expression level of the three biomarkers

To further evaluate the expression pattern of the 3 genes, we verified their expression in the validation sets. It was discovered that SLC8A2, ATP2B3 and SRCIN1 were also remarkably downregulated in GSE7696 (Fig. 4A). Besides, the decrease in the expression of SLC8A2, ATP2B3 and SRCIN1 for glioma group from TCGA database again verified our results (Fig. 4B). Our findings emphasized the underlying potential of SLC8A2, ATP2B3, and SRCIN1 as novel diagnostic biomarkers for glioma patients.

3.4 The relationship between the expression of three biomarkers and the clinical features of glioma

Considered the complete clinical information and survival information of the patient in the TCGA database, clinical data for gliomas from the TCGA database were obtained for analysis. We investigated the differential expressions of ATP2B3, SLC8A2, and SRCIN1 in different clinical features of gliomas. The results demonstrated a statistically significant difference in expression between WHO grade II and WHO III gliomas, and the expression of ATP2B3, SLC8A2, and SRCIN1 reduced considerably with WHO grade increased (Fig. 5A). IDH was categorized into wild type (WT) and mutant type (Mut) by the WHO for gliomas, there were statistically significant differences in ATP2B3, SLC8A2, and SRCIN1 expression between the two groups (Fig. 5B). Besides, ATP2B3 and SLC8A2 were increased in the 1p/19q codeletion group than in the no-codeletion group, but SRCIN1 demonstrated the opposite expression pattern (Fig. 5C). Furthermore, SLC8A2 and SRCIN1 expression levels were higher in patients over 60 years old than in those under 60 years old, although SRCIN1 was higher in patients under 60 years old (Fig. 5D).

3.5 The relationship between the expression of three biomarkers and prognosis in glioma patients

Next, we first performed univariate Cox regression analysis in TCGA glioma patients, and the results demonstrated that WHO grade (G3&G4), 1p/19q non-codeletion, wildtype IDH status, age > 60 years old, and high expression of ATP2B3, SLC8A2 and SRCIN1 were significantly associated with the prognosis of glioma patients (Fig. 6A). Additional multivariate Cox regression demonstrated that these variables are independent prognostic factors for gliomas (Fig. 6B). To further investigate the impact of ATP2B3, SLC8A2, and SRCIN1 expression on the prognosis of glioma patients, the Kaplan–Meier survival curve was used to assess overall survival (OS), disease-free survival (DSS), and progression-free survival (PFS) in TCGA glioma patients. Patients with high ATP2B3 expression had significantly longer OS, DSS,

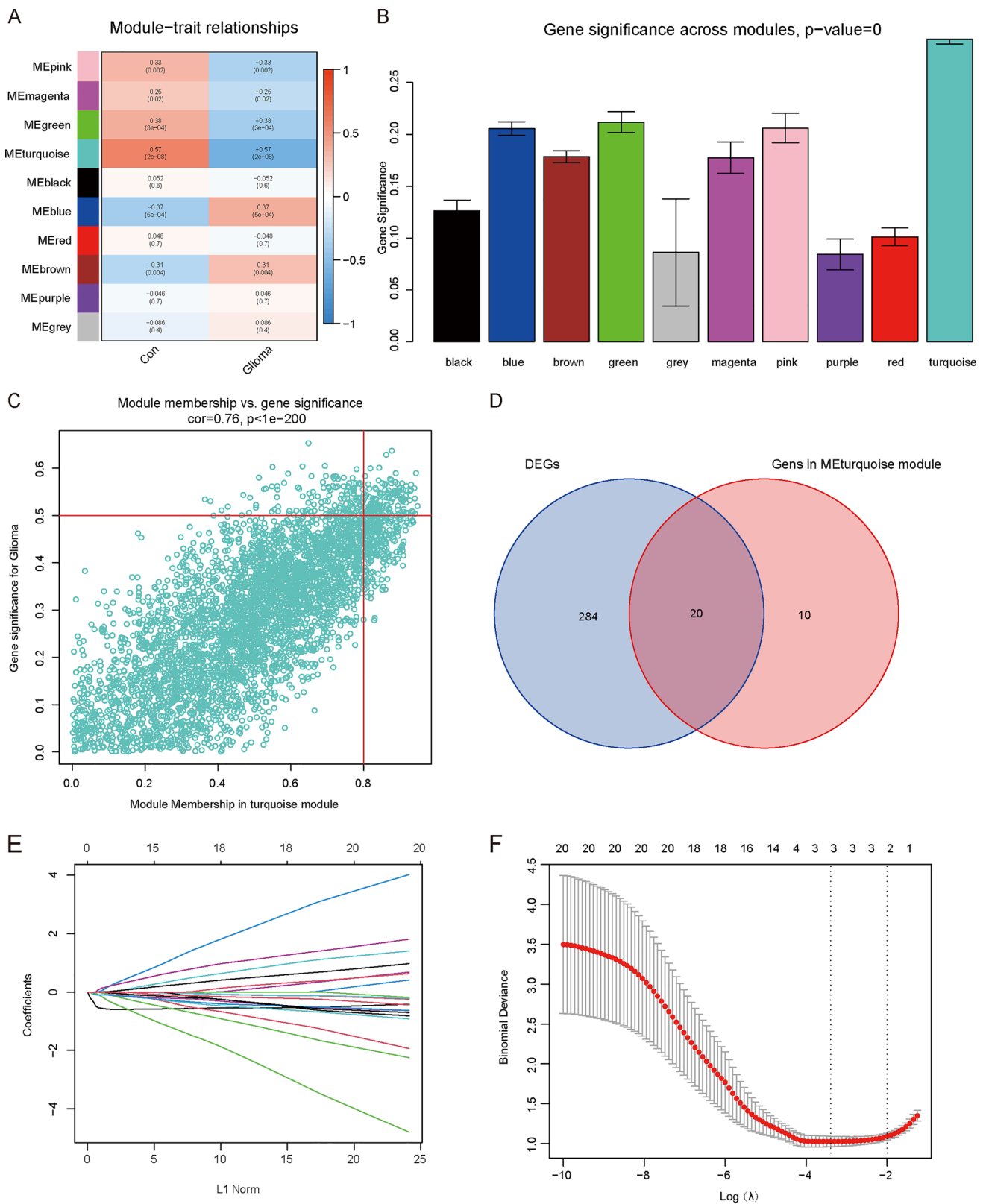


Fig. 3 Identification of the 3 biomarkers by WGCNA and LASSO regression analysis. **A** The heat map of the relationship between module and clinical trait. **B** Distribution of mean gene significance in distinct modules. **C** The scatter plot displayed the correlation between the hub module and gene significance. **D** The 20 Overlapping genes between DEGs and the “MEturquoise” module. **E** LASSO coefficient profiles of the 20 genes. **F** The optimal value of $\log(\lambda)$ indicated 3 hub genes as independent diagnostic factors

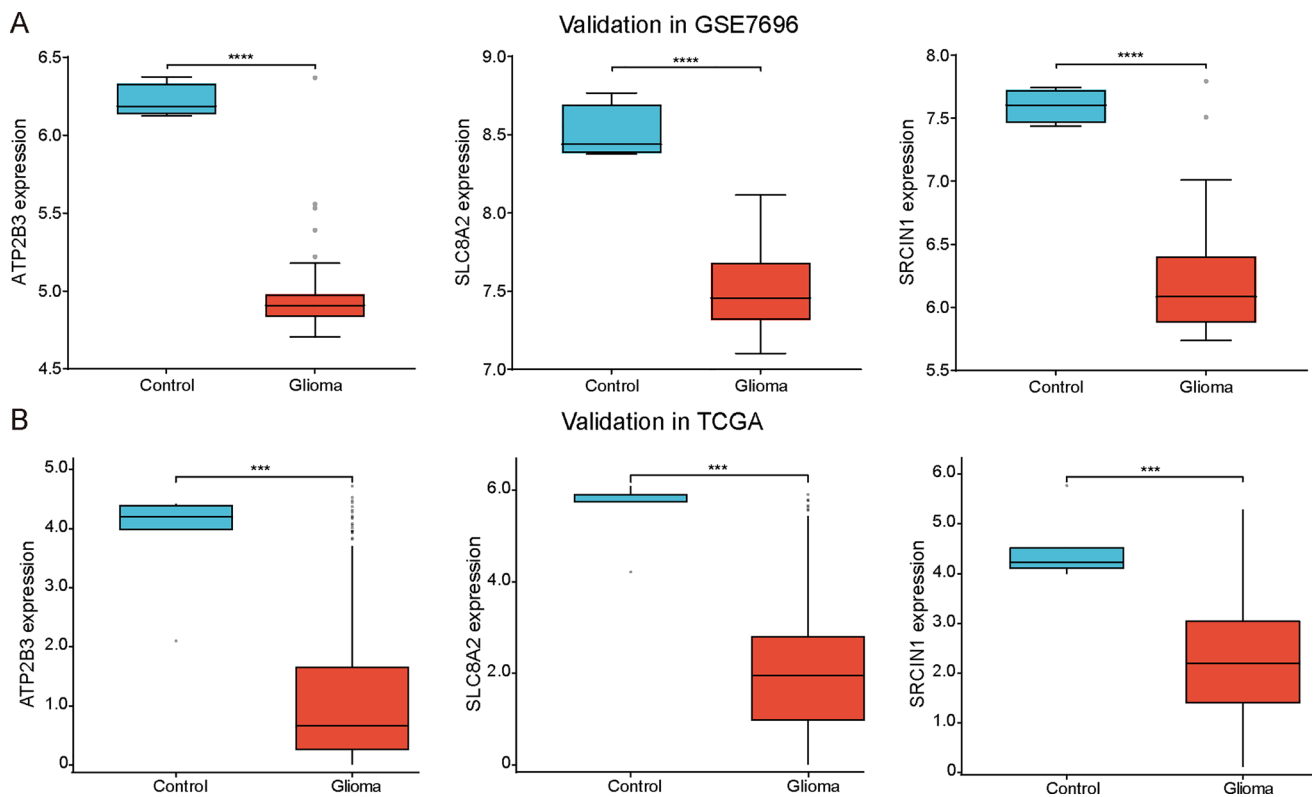


Fig. 4 Validation of expression level and diagnostic ability of the biomarkers. **A** The expressing pattern of the 3 genes in glioma samples and normal samples from GSE7696. **B** The expressing pattern of the 3 genes in glioma samples and normal samples from TCGA. Statistics performed by Mann Whitney test, * $P < 0.05$, ** $P < 0.01$, *** $P < 0.001$

and PFS than those with low ATP2B3 expression (Fig. 6C). Besides, the OS, DSS, and PFS of patients with high SLC8A2 expression were considerably longer than those of patients with low ATP2B3 expression (Fig. 6D). Similarly, elevated SRCIN1 expression also extended OS, DSS, and PFS in glioma patients (Fig. 6E).

3.6 Prediction of anticancer drugs sensitivity based on the expression of 3 biomarkers

Due to glioma heterogeneity and individual variation, standard treatment might not be effective for all patients. Therefore, one of the greatest obstacles to the effective treatment of gliomas is figuring out their unique molecular properties. Therefore, we used the Cellminer database to inquire about the connection between 3 hub genes and chemo drug sensitivity in this study (Fig. 7). The expression of SRCIN1 was positively correlated with the sensitivity of Hydrastinine HCL, APR-246, R-306465, PF-06747775, Abexinostat, AZD-9496, and Pracinostat. While the sensitivity of AMD-070, BAY-1251152, SOMCL-12-81, VX-322, Zoledronate, dimethylfasudil, and SGX-523 were negatively correlated with SRCIN1 expression. In addition, Mitomycin and JNJ-4717096 sensitivity were positively related to ATP2B3 expression, while sensitivity to BMS-986158, BLU-285, AT-13148, I-BET-151, SHP-099, cs-1730, and AZD-5153 were negatively correlated with ATP2B3 expression. Moreover, the higher the expression of SLC8A2, the worse the sensitivity of glioma patients to I-BET-151, SHP-099, cs-1730, BMS-986158, and AZD-5153.

3.7 Associations between immune cell infiltration and biomarkers

The infiltration of immune cells in tumors is closely related to clinical outcomes, so infiltrated immune cells in tumors might be potential drug targets to improve patient survival. Firstly, the ssGSEA algorithm was performed to investigate the immune landscape for patients in GSE50161 and GSE188256. The heat maps unveiled the distinct immune cell infiltration pattern in glioma samples compared to the normal control (Fig. 8A). Activated CD4 T cell, activated

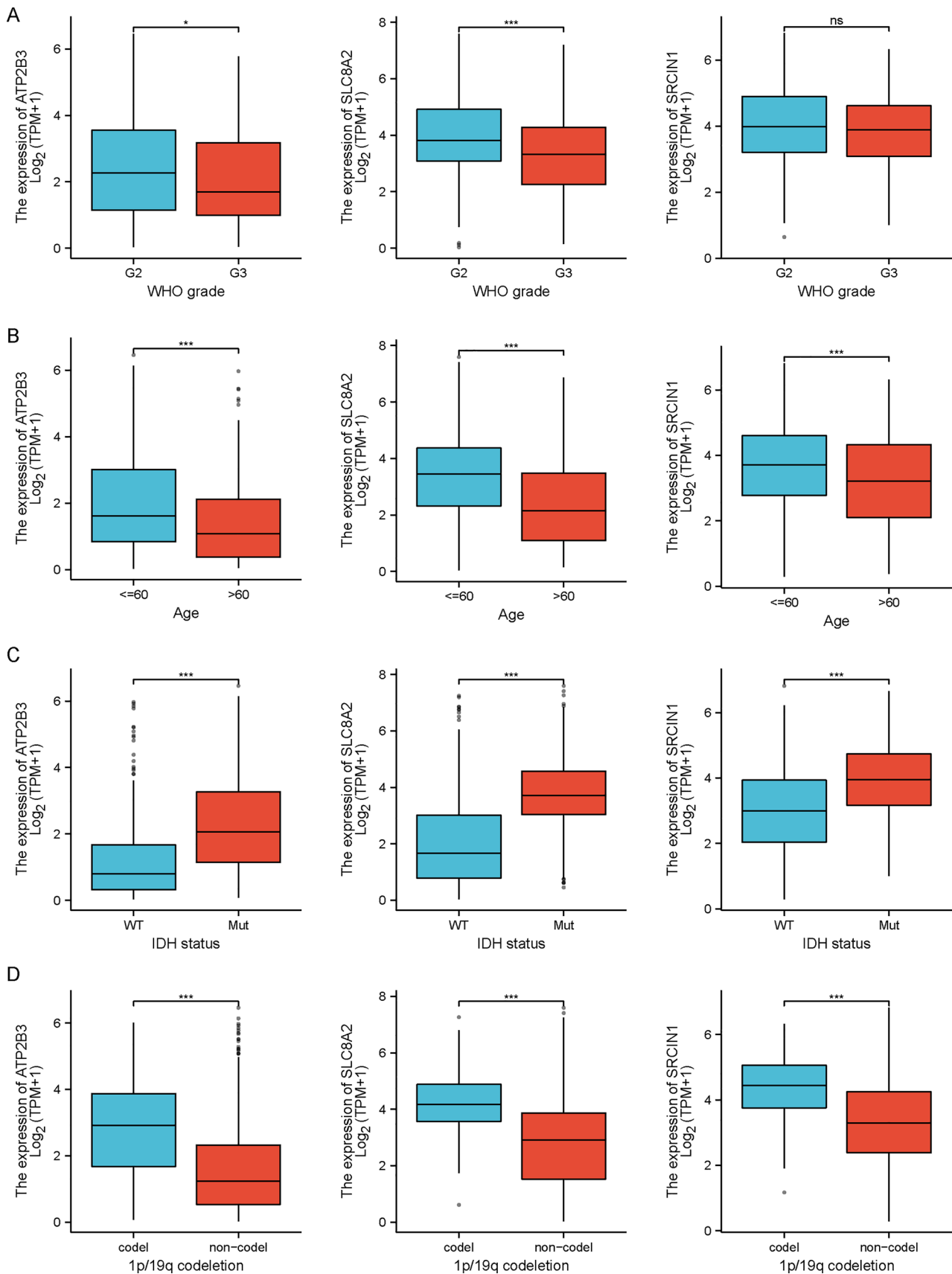


Fig. 5 Distribution of the 3 genes' expression in different clinicopathological groups. **A** WHO grades. **B** Age. **C** IDH status. **D** 1p/19q codeletion. Statistics performed by Mann Whitney test, *P < 0.05, **p < 0.01, ***p < 0.001

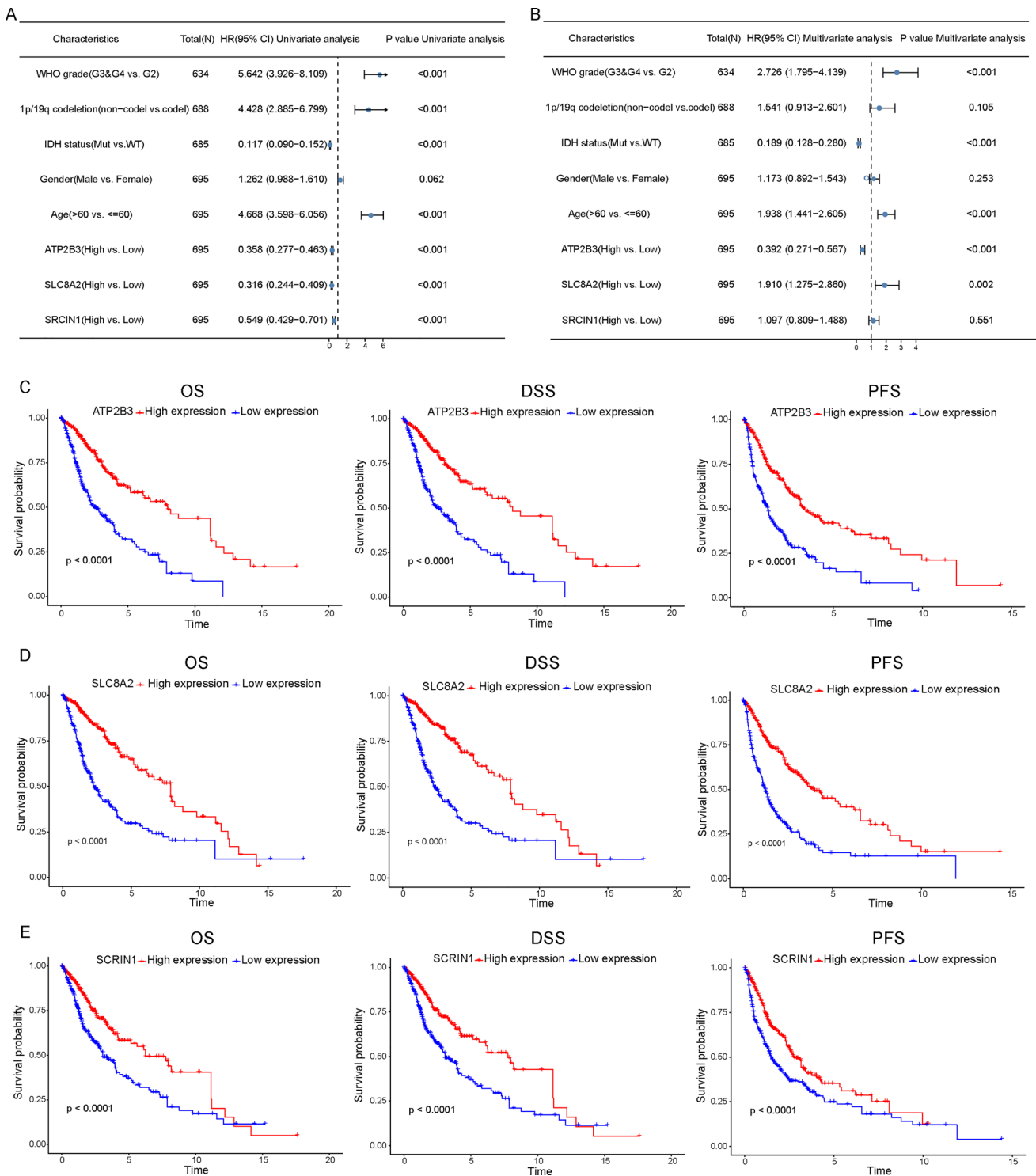


Fig. 6 Association between the expression of the 3 biomarkers and prognosis of glioma patients. **A** Univariate regression analysis on the 3 biomarkers and different clinicopathological factors. **B** Multivariate regression analysis on the 3 biomarkers and different clinicopathological factors. **C** Differences in OS, DSS, and PFS between patients with high and low ATP2B3 expression. **D** Differences in OS, DSS, and PFS between patients with high and low SLC8A2 expression. **E** Differences in OS, DSS, and PFS between patients with high and low SRCIN1 expression

CD8T cell, activated dendritic cell, CD56 bright natural killer cell, gamma delta.T cell, immature B cell, MDSC, macrophage, mast cell, natural killer T cell, neutrophil, regulatory T cell, T.follicular helper cell, type 1 T helper cell, type

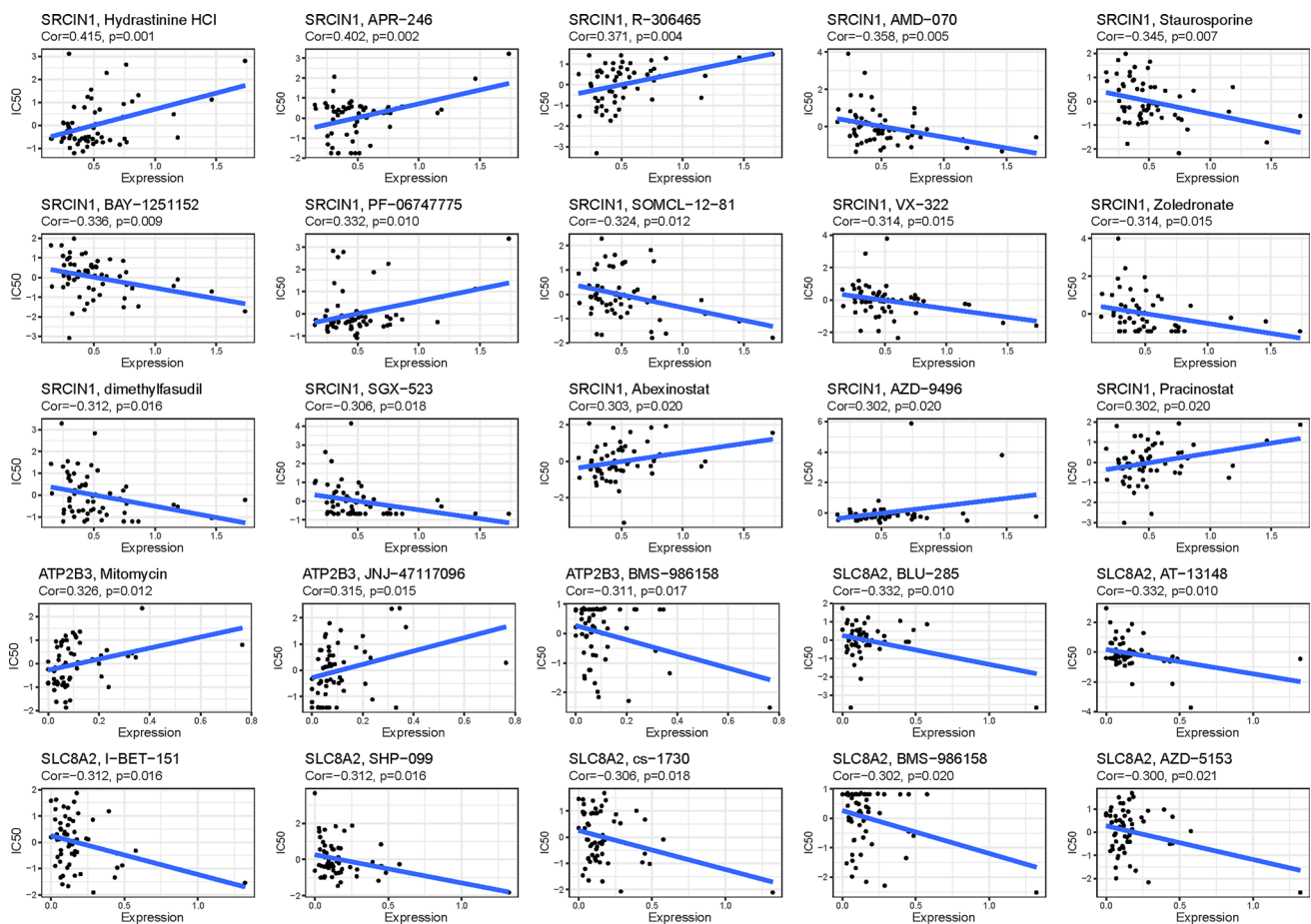


Fig. 7 Prediction of anticancer drug sensitivity based on biomarkers. The relationship between the IC₅₀ of anticancer drugs and the expression of the 3 biomarkers

17 T helper cell, type 2 T helper cell levels were all dramatically increased in the tumor samples than in control samples (Fig. 8B), indicating their nonnegligible function in the development of glioma. The correlations between the three biomarkers and different immune cells were calculated using spearman correlation analysis. It can be found that the three biomarkers are negatively associated with most of the immune cells, this was consistent with their low expression in gliomas (Fig. 8C).

Then the immune infiltration scene had also been revealed in TCGA database. The fraction of 22 infiltrating immune cells in the TCGA cohort was displayed in Fig. 9A. The CIBERSORT algorithm showed the proportion of infiltrated immune cell in high-expressed and low-expressed biomarker groups, T cells regulatory (Tregs), macrophages M2, dendritic cells activated and Neutrophils were increased in low-ATP2B3, low-SLC8A2 and Low-SRCIN1 groups (Fig. 9B–D). The expression of infiltrated immune cell in high-expressed and low-expressed biomarker groups was further analyzed by ssGSEA algorithm, most infiltrated immune cell including activated B cells, activated CD4 cells, activated CD8 cells, macrophage, MDSC, T follicular helper cell, type 1 T helper cell and type 17 T helper cell were negatively correlated with the expression of the three biomarkers (Fig. 9E–G). Both methods confirmed a significant correlation between the infiltration of immune cells and the expression of three biomarkers. Additionally, we found a significant correlation between the expression levels of the immune checkpoint genes CTLA4, PDCD1, and PDCD1LG2 and the expression of the three biomarkers. These genes tended to be expressed at higher levels in the Low-SLC8A2, Low-ATP2B3, and Low-SRCIN1 groups (Fig. 10A–C).

3.8 Verification of expression and biological function of the 3 biomarkers

Based on the immunohistochemical staining results from the HPA databases, the expression levels of SLC8A2, ATP2B3, and SRCIN1 were evaluated. These three genes were found to be down-regulated in gliomas compared to normal brain tissue. SLC8A2 and ATP2B3 exhibited medium staining levels, while SRCIN1 showed low staining compared to normal

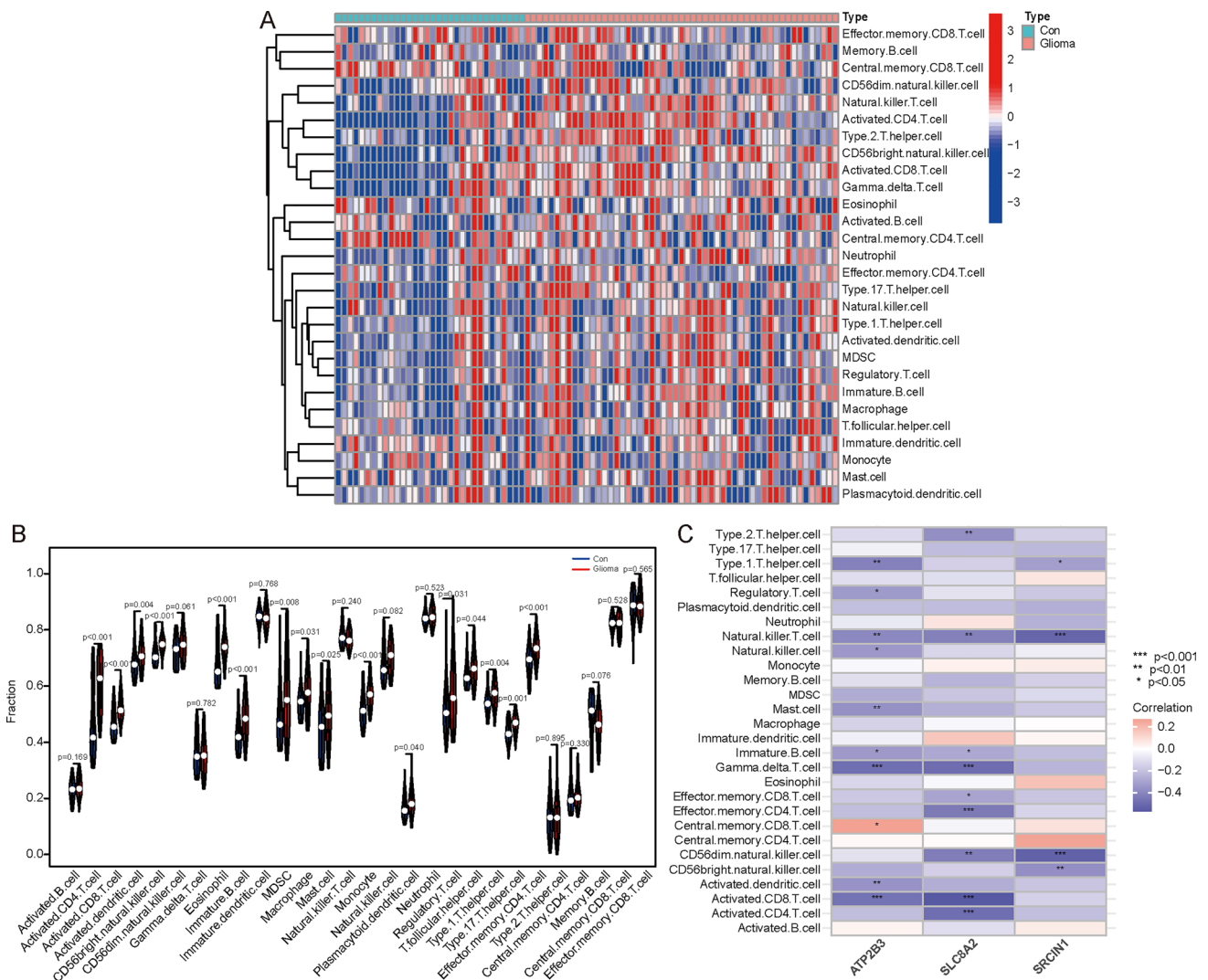


Fig. 8 The distribution of immune landscape related to glioma in GEO cohort. **A** Heatmap and **B** violin plot demonstrated the relative concentration of 28 immune cells in normal samples and glioma samples. **C** The associations between immune cell infiltration and the 3 biomarkers. Statistics performed by Mann Whitney test, *P < 0.05, **P < 0.01, ***P < 0.001

brain tissue (Fig. 11A). To validate these findings, we also assessed the expression levels of ATP2B3 and SRCIN1 using immunofluorescence in our own collected patient samples. Consistently, both ATP2B3 (Fig. 11B) and SRCIN1 (Fig. 11C) showed reduced fluorescence staining in glioma tissue, matching the results obtained from the HPA database.

To further investigate the roles and predictive value of SLC8A2, ATP2B3, and SRCIN1, qRT-PCR and Western Blot analyses were performed to assess their expression at the mRNA and protein levels in different glioma cell lines. The expression of these three genes was found to be reduced in both T98G and U251 glioma cell lines, consistent with the previous findings (Fig. 12A–C). Subsequently, we overexpressed these three genes in each of the two cell lines to observe their effects on tumor proliferation and migration. Flow apoptosis assay revealed a significant increase in the percentage of early apoptotic cells in both glioma cell lines after the overexpression treatment (Fig. 12D). CCK8 assay demonstrated that overexpression of SLC8A2, ATP2B3, and SRCIN1 inhibited the growth of T98G and U251 cells (Fig. 12E). Scratch assays confirmed that the overexpression of these three genes reduced the migration of glioma cells (Fig. 13A). Transwell assay suggested that the invasive ability of glioma cell lines was also significantly reduced after the overexpression treatment (Fig. 13B). These results

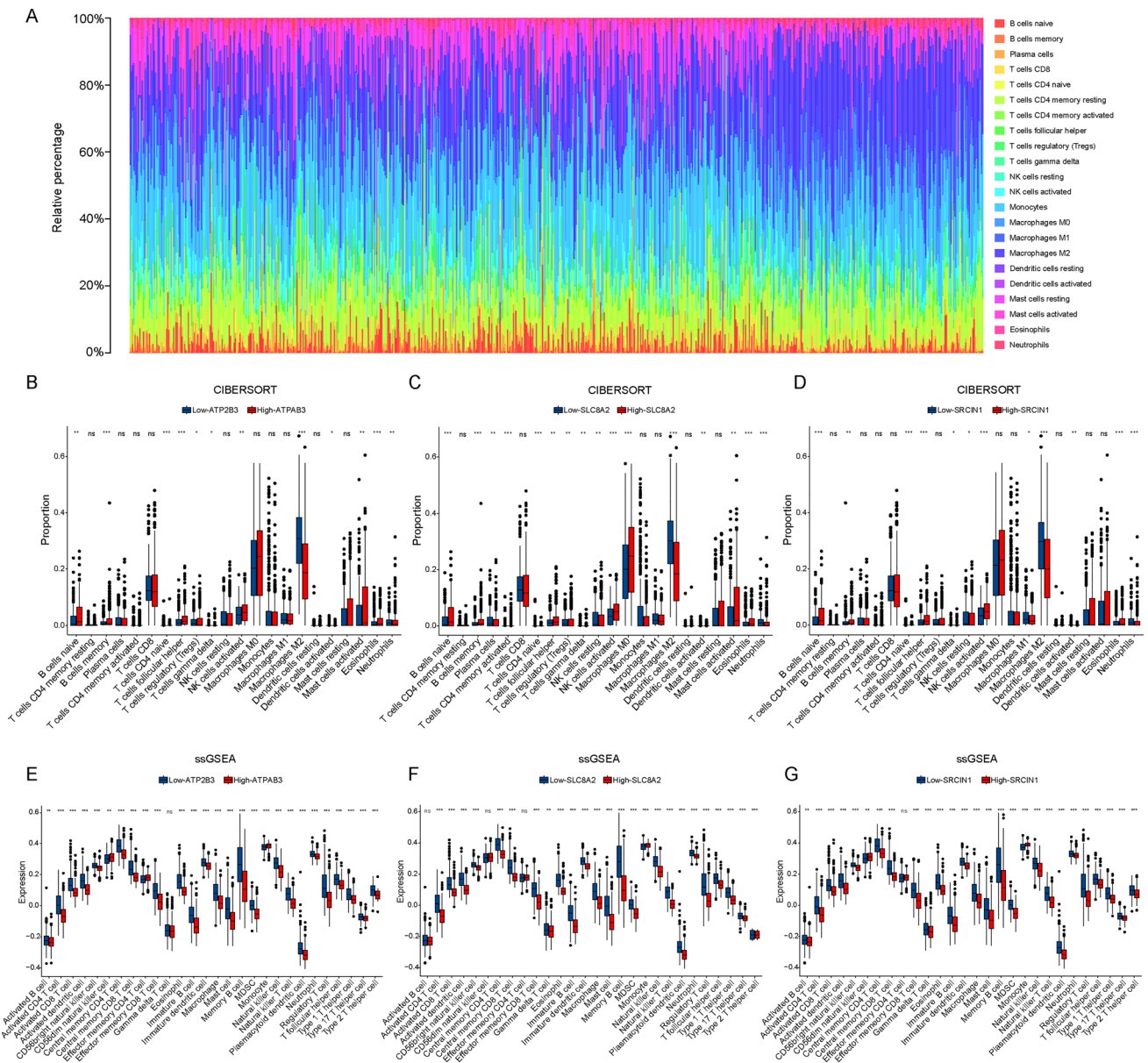


Fig. 9 The distribution of immune landscape related to glioma in TCGA cohort. **A** Composition of immune cells in tumor and normal samples in TCGA. **B–D** Proportion of infiltrated immune cells in high-expressed and low-expressed biomarker groups by CIBERSORT algorithm. **E–G** Expression of infiltrated immune cells in in high-expressed and low-expressed biomarker groups by ssGSEA algorithm. Statistics performed by Mann Whitney test, * $P < 0.05$, ** $P < 0.01$, *** $P < 0.001$

indicate that the downregulation of SLC8A2, ATP2B3, and SRCIN1 promotes glioma proliferation and migration, thus facilitating glioma progression in vivo.

These findings suggested that SLC8A2, ATP2B3, and SRCIN1 were the underlying biomarkers for glioma.

4 Discussion

Glioma is the most prevalent primary malignant brain tumor in adults [23, 24]. Based on tumor growth patterns and the presence or absence of IDH mutations, the WHO categorized confined gliomas (WHO grade I) and diffuse invasive gliomas (WHO grade II-IV) [25]. WHO grade IV GBM had worse median survival compared with WHO II-III gliomas

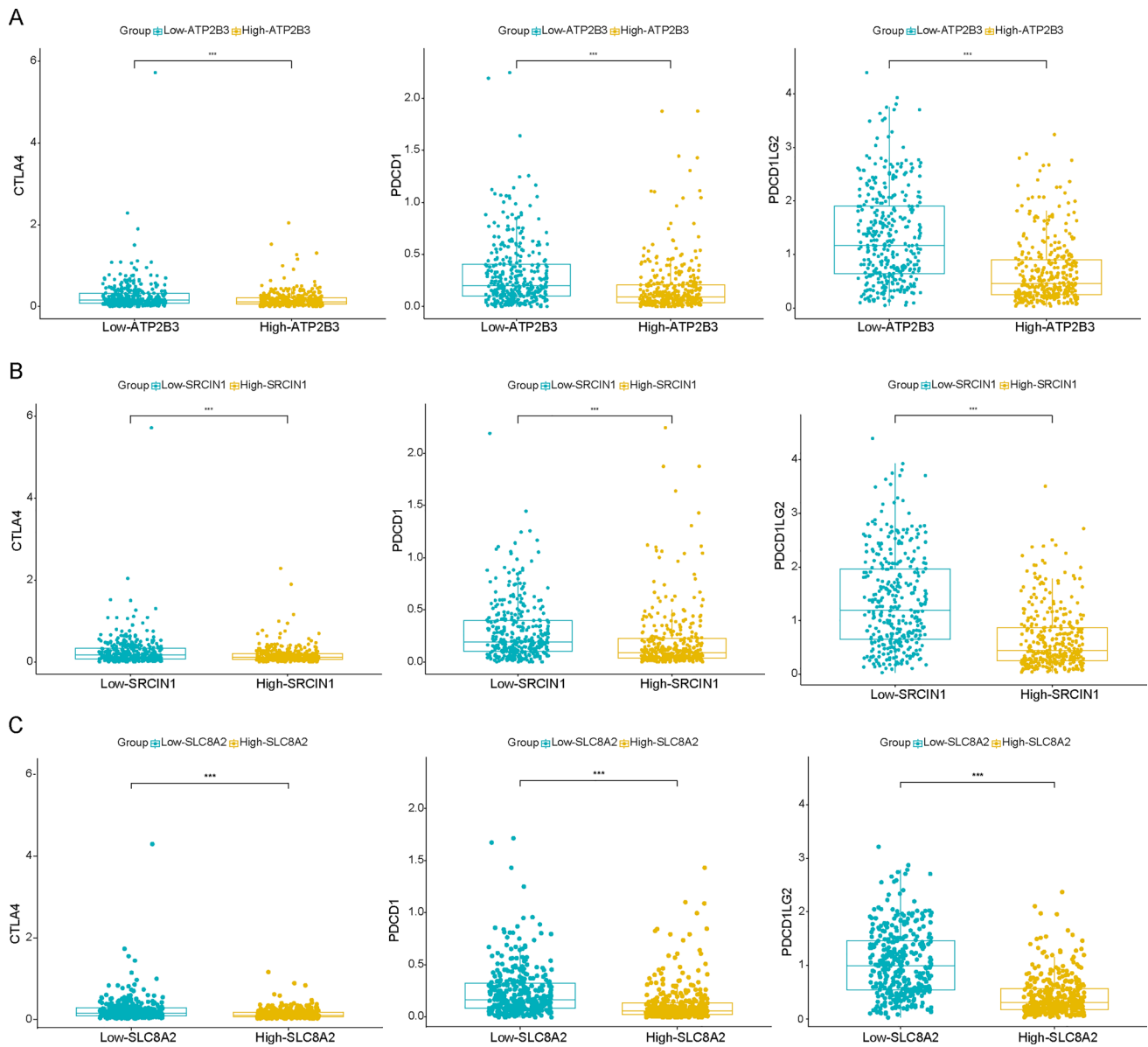


Fig. 10 Correlation between the immune checkpoint genes and the three biomarkers. **A** The expression of immune checkpoint genes CTLA4, PDCD1, and PDCD1LG2 in Low-ATP2B3 and High-ATP2B3 groups. **B** The expression of immune checkpoint genes CTLA4, PDCD1, and PDCD1LG2 in Low-SRCIN1 and High-SRCIN1 groups. **C** The expression of immune checkpoint genes CTLA4, PDCD1, and PDCD1LG2 in Low-SLC8A2 and High-SLC8A2 groups. Statistics performed by Mann Whitney test, * $P < 0.05$, ** $P < 0.01$, *** $P < 0.001$

[26]. Therefore, feasible biomarkers for early detection of glioma might be advantageous for patient management and prognosis.

As direct, rapid, and effective diagnostic tools, biomarkers play an important role in the diagnosis, progression, treatment, and drug efficacy monitoring of disease, and they are also significant drug development targets [27]. Multimodal genetic, molecular, and radiological histology could predict the prognosis of glioma patients, whereas targeted therapy and individualized treatment are increasingly being offered for diverse patients [28]. Molecular diagnostics and personalized treatment ameliorate the options for the management of glioma patients [29]. Some identified biomolecular markers have been proven for their availability in the molecular pathological categorization of gliomas, although clinical investigations of targeted medications connected with them have shown inconsistent results. In addition, it is improbable that a single marker can be utilized to stratify all glioma subtypes prospectively. Consequently, the use of molecular profiling to investigate novel biomarkers as a supplement may provide more precise and valuable clinical insights.

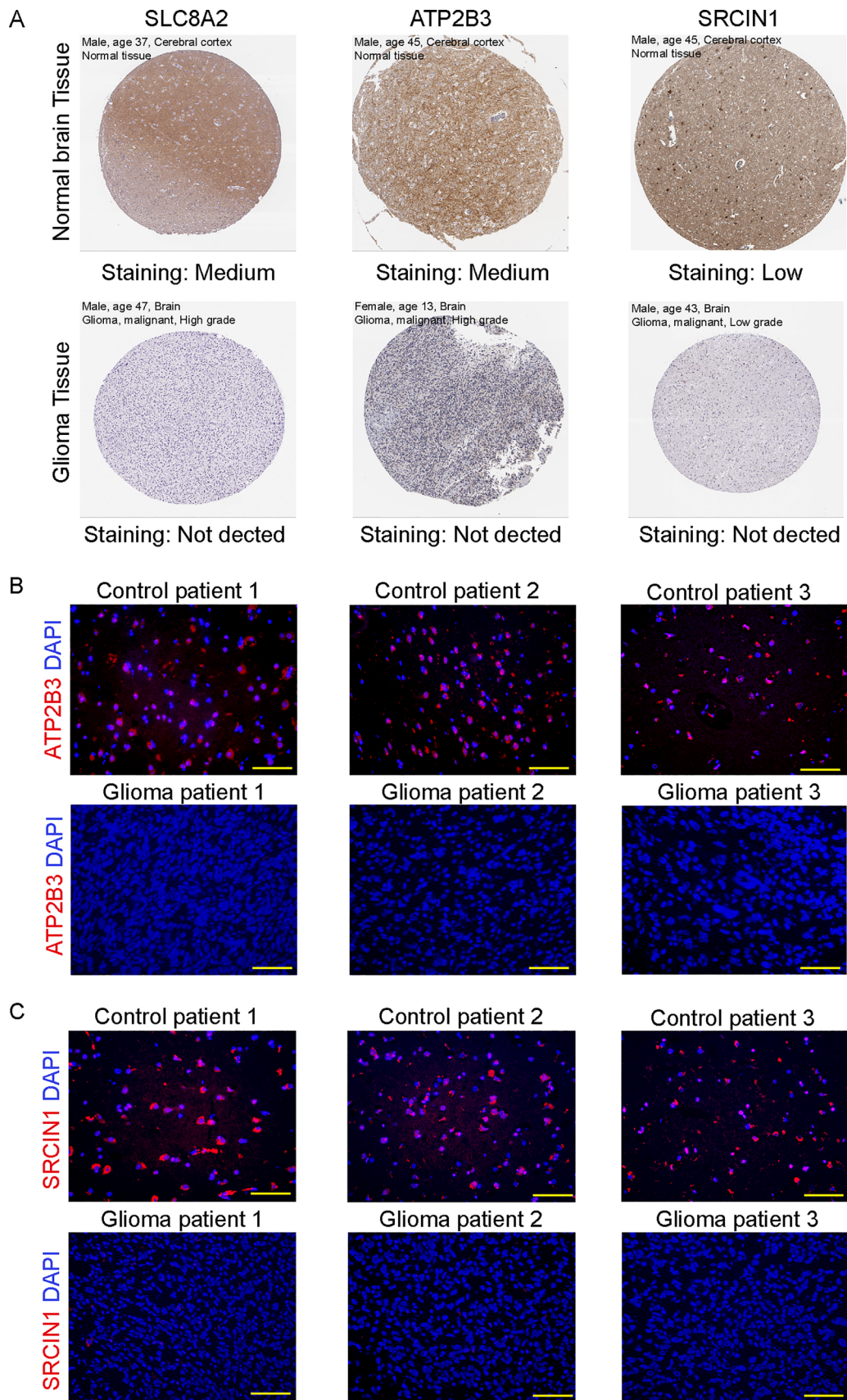


Fig. 11 External validation of protein expression levels for the 3 biomarkers. **A** The expression of SLC8A2, ATP2B3, and SRCIN1 protein levels in the HPA database. **B** The expression ATP2B3 protein levels in our cohort. **C** The expression SRCIN1 protein levels in our cohort. Scale bars represent 50 μ m

Fig. 12 Verification of expression of the 3 biomarkers in glioma cell lines. **A** The expression of the 3 genes in T98G and U251 glioma cell lines. **B** Semiquantitative analysis of gray scale values. **C** Relative mRNA expression of the 3 genes in T98G and U251 glioma cell lines. **D** Apoptosis analysis in the overexpression experiments. **E** Cell growth analysis in the overexpression experiments. n = 3 per group in **A–E**. Statistics performed by one-way ANOVA, *P < 0.05, **P < 0.01, ***P < 0.001

WGCNA could detect relevant, dense correlation modules linked with specific clinical characteristics, which is valuable for inferring the progress of tumor growth and providing novel targets to inhibit crucial signaling pathways [30–32]. LASSO is a machine learning-based algorithm for screening characteristic variables in clinical decision-making [33–35]. Numerous studies have documented the application of WGCNA and LASSO regression in glioma, respectively, however, studies combining the two approaches to uncover biomarkers for glioma are still infrequent.

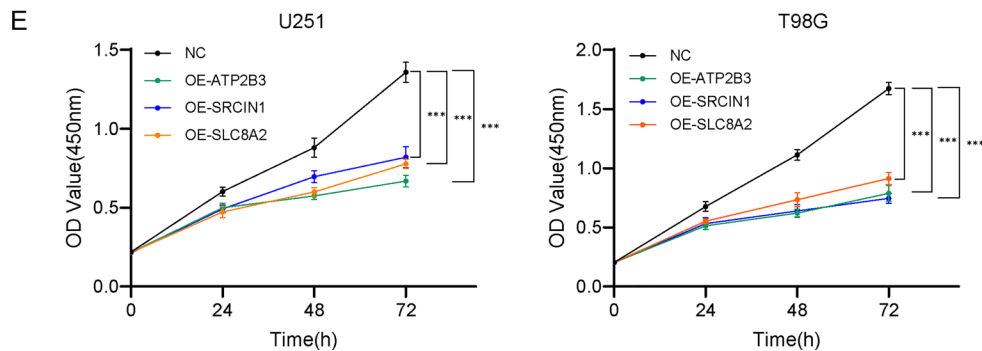
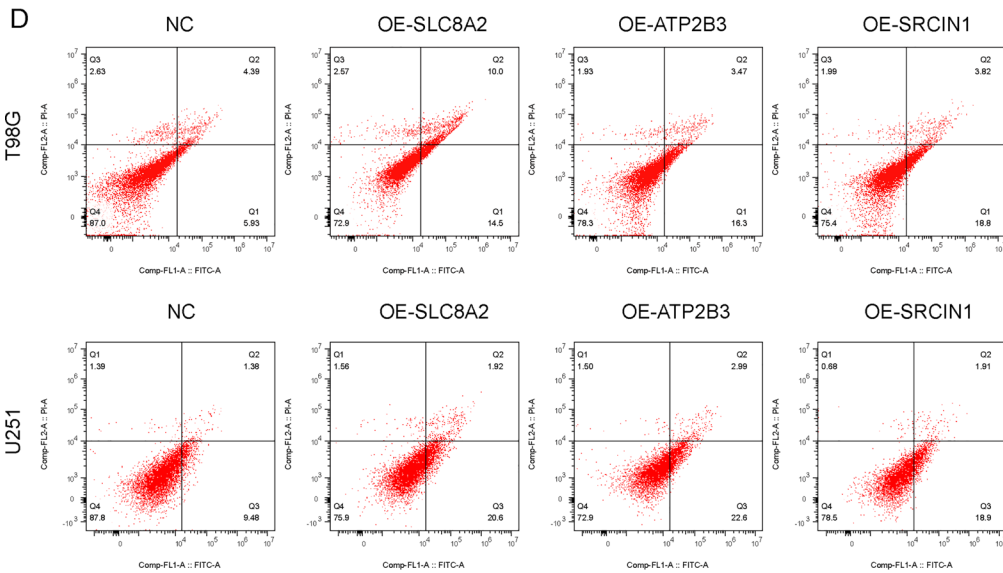
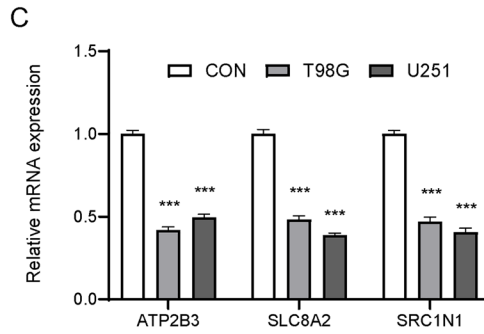
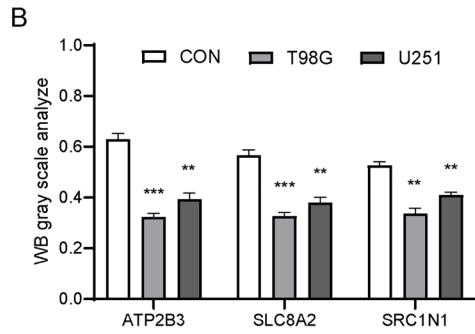
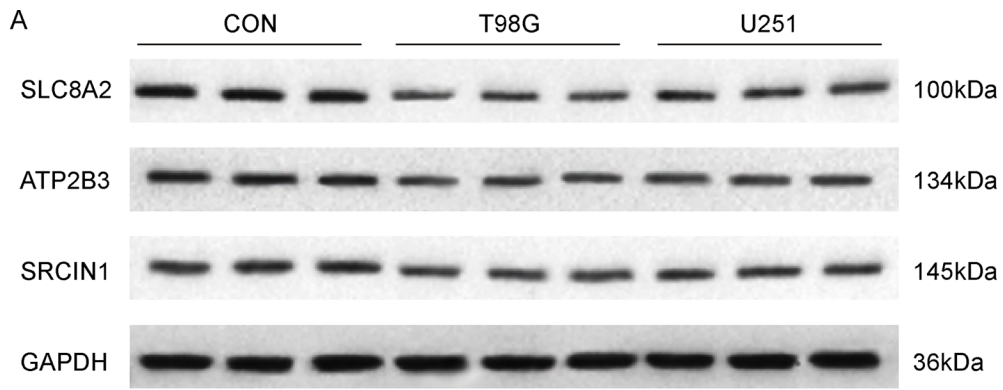
In the present study, we identified 3 hub genes through the combination of WGCNA and LASSO regression, namely SLC8A2, ATP2B3, and SRCIN1. It is possible to determine that the expression of these three biomarkers was being suppressed in the tumor group compared to the normal control group in multiple-database. Secondly, we further proved that SLC8A2, ATP2B3, and SRCIN1 were capable of serving as independent glioma predictors. The expression of 3 biomarkers was highly linked with overall survival (OS), disease-specific survival (DSS), and progression-free survival (PFS). Thirdly, there was a strong correlation between the sensitivity of anticancer medicines and the expression of biomarkers. Additionally, a close relationship was also discovered between the three biomarkers and most tumor immune cells. Ultimately, immunostaining of the three biomarkers in our cohort and in vitro cell experiments further confirmed their diminished expression in glioma tissue.

These three genes have been the subject of a number of researches that have reported on their involvement in gliomas. SLC8A2 had been found to play a significant role in the process of DNA methylation in gliomas [36]. Another study suggested that SLC8A2 might function as a tumor suppressor, preventing the invasion, angiogenesis, and growth of glioblastoma [37]. Current studies of ATP2B3 have been discovered to be mainly related to aldosterone adenomas [38–40], and there were no studies related to gliomas. SRCIN1 was considered one of the genes closely associated with clinical factors and tumor microenvironment in gliomas [41]. In addition, SRCIN1 had been found to be an independent risk factor inversely associated with the aggressiveness of neuroblastoma, this suggested that SRCIN1 might serve as a new independent prognostic marker for patient prognosis and treatment [42]. In conclusion, it can be discovered the inhibited expression of the three hub genes in glioma might enhance the invasion and progression of glioma.

Tumor-infiltrating immune cells are an essential component of the tumor microenvironment (TME), which plays a crucial role in tumor development and progression. Tumor-derived cytokines and chemokines further modify invading immune cells, causing them to develop tumor-specific functional phenotypes and ultimately become tumor-associated immune cells. As a result, the inflammatory or anti-inflammatory responses induced by these tumor-associated immune cells may have significant implications on glioma growth, recurrence, and treatment resistance. The glioma microenvironment contains a variety of immune cells, including MDSCs, natural killer cells (NK cells), macrophages, neutrophils, CD4 + helper T cells (Ths), CD8 + cytotoxic T lymphocytes (CTLs), and regulatory T (T reg) cells [43, 44]. Therefore, we further analyzed the correlation between the three biomarkers and immune cell infiltration and found that the expression of the three biomarkers were negatively correlated with most immune cells, including activated B cells, activated CD4 cells, activated CD8 cells, macrophage, MDSC, T follicular helper cell, type 1 T helper cell and type 17 T helper cell, which coincided with clinical practice and some research results [45, 46]. This also highlights the potential role of the three biomarkers as immunotherapy targets for glioma.

Immunohistochemical staining results from the HPA databases and immunofluorescence analysis of our own collected patient samples suggested that the decreased expression of these genes may be associated with the development and progression of gliomas. Besides, the consistent reduction in their expression levels in T98G and U251 cell lines suggested that this downregulation may be a common feature in glioma cells. The increased apoptosis, decreased cell growth, reduced migration, and invasive ability observed in the overexpression experiments suggested that the downregulation of these genes may contribute to the aggressive behavior of gliomas.

Despite the use of several bioinformatics and statistical techniques, there were still some limitations and shortcomings. First of all, the data in the GEO database used in this study were small in sample size, thus sequencing data or clinical data of larger samples are required. Secondly, this study only verified the feasibility of the three genes through bioinformatics and molecular biology experiments, relevant clinical research is essential in the future. Next, in clinical diagnosis and treatment, histology, molecular testing and precision therapy should be dynamically combined and complementary. Finally, there are few molecular markers to maintain stability due to



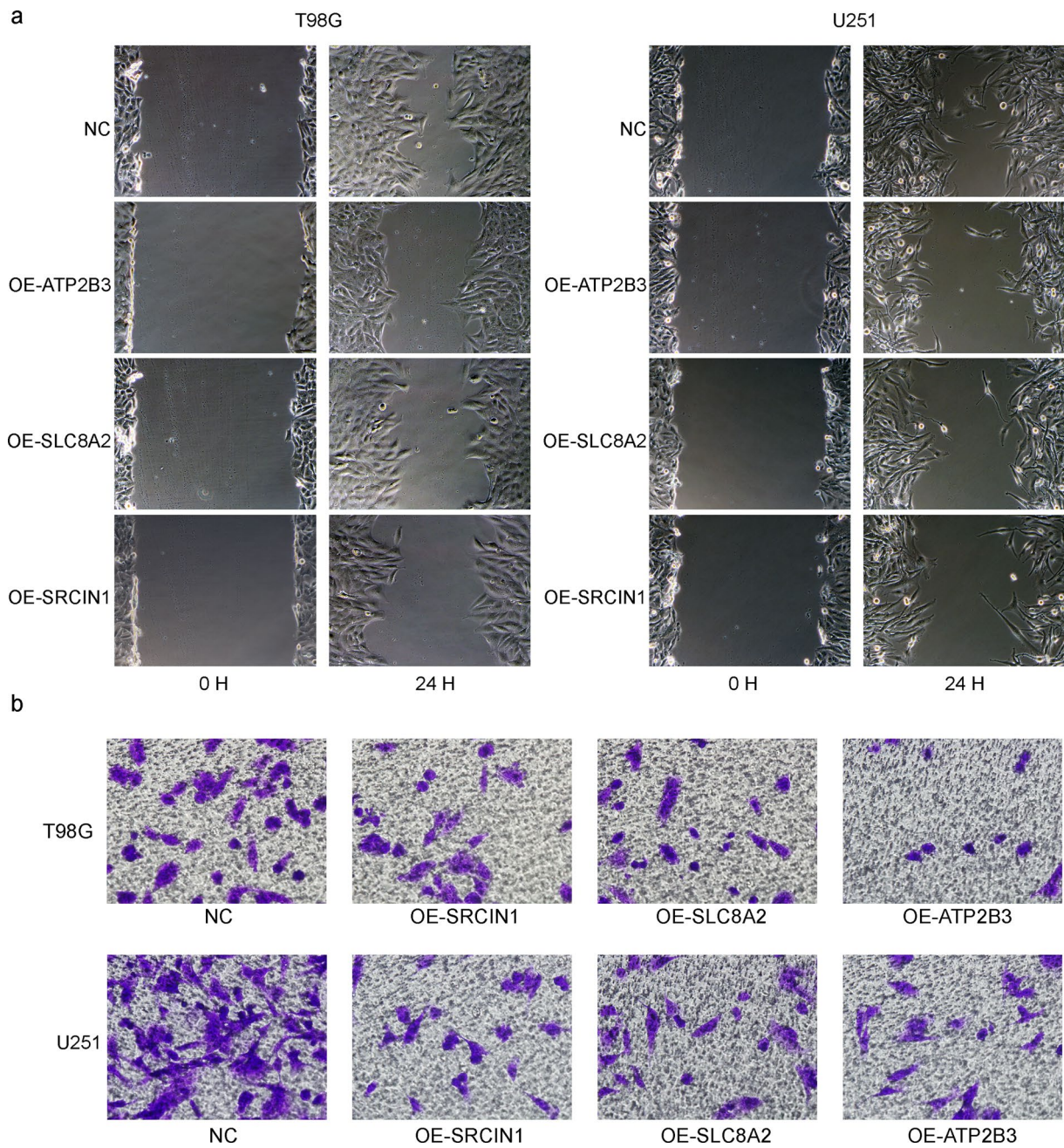


Fig. 13 Verification of biological function of the 3 biomarkers in glioma cell lines. **A** Scratch assay in the overexpression experiments. **B** Transwell invasion assay in the overexpression experiments. $n=3$ per group. Statistics performed by one-way ANOVA, $*P < 0.05$, $**P < 0.01$, $***P < 0.001$

the continuous evolution of tumors, so we cannot ignore the consequent changes in molecular markers that occur during the dynamic development of gliomas. Further research is needed to elucidate the underlying mechanisms and explore their potential clinical applications in glioma diagnosis and treatment.

5 Conclusion

In summary, the three novel hub genes including SLC8A2, ATP2B3, and SRCIN1 are found to be promising biomarkers for individualized diagnosis and management of glioma. This strengthens molecular diagnostics and individualized treatment in neuro-oncology.

Acknowledgements Not applicable.

Author contributions Y.H.Z. and C.J.S. designed the study. Y.H.Z. and C.J.S. participated in the bioinformatics and statistical analysis. X.J. and Y.Z. did the immunohistochemistry analysis and figure editing, and X.L.X revised the manuscript. All authors contributed to the article and approved the submitted version.

Funding This article was supported by the Foundation of Hunan Science and Technology Department-Clinical Medical Technology Demonstration Base for Neurosurgery in Hunan Province (2018SK4003).

Data availability The datasets containing normal and tumor samples were downloaded from the GEO database (www.ncbi.nlm.nih.gov/geo) and TCGA database (<https://cancergenome.nih.gov/>).

Declarations

Ethics approval and consent to participate Human participants included in this study were reviewed and approved by the Medical Ethics Committee of The First People's Hospital of Changde City. The patients provided their written informed consent to participate in this study. Information on the brain tissue section samples was provided in supplementary material. The Ethics approval number was YX-2023-234-01.

Consent for publication Written informed consent had been obtained from the patient for publication of this study and any accompanying images.

Competing interests The authors declare no competing interests.

Open Access This article is licensed under a Creative Commons Attribution-NonCommercial-NoDerivatives 4.0 International License, which permits any non-commercial use, sharing, distribution and reproduction in any medium or format, as long as you give appropriate credit to the original author(s) and the source, provide a link to the Creative Commons licence, and indicate if you modified the licensed material. You do not have permission under this licence to share adapted material derived from this article or parts of it. The images or other third party material in this article are included in the article's Creative Commons licence, unless indicated otherwise in a credit line to the material. If material is not included in the article's Creative Commons licence and your intended use is not permitted by statutory regulation or exceeds the permitted use, you will need to obtain permission directly from the copyright holder. To view a copy of this licence, visit <http://creativecommons.org/licenses/by-nc-nd/4.0/>.

References

1. Weller M, Wick W, Aldape K, Brada M, Berger M, Pfister SM, et al. Glioma. *Nat Rev Dis Prim.* 2015;1:15017.
2. Sanai N, Alvarez-Buylla A, Berger MS. Neural stem cells and the origin of gliomas. *N Engl J Med.* 2005;353:811–22.
3. Dunn GP, Rinne ML, Wykosky J, Genovese G, Quayle SN, Dunn IF, et al. Emerging insights into the molecular and cellular basis of glioblastoma. *Genes Dev.* 2012;26:756–84.
4. Tan AC, Ashley DM, López GY, Malinzak M, Friedman HS, Khasraw M. Management of glioblastoma: state of the art and future directions. *CA Cancer J Clin.* 2020;70:299–312.
5. Perry JR, Laperriere N, O'Callaghan CJ, Brandes AA, Menten J, Phillips C, et al. Short-course radiation plus temozolomide in elderly patients with glioblastoma. *N Engl J Med.* 2017;376:1027–37.
6. Bi J, Chowdhry S, Wu S, Zhang W, Masui K, Mischel PS. Altered cellular metabolism in gliomas—an emerging landscape of actionable co-dependency targets. *Nat Rev Cancer.* 2020;20:57–70.
7. Berger TR, Wen PY, Lang-Orsini M, Chukwueke UN. World Health Organization 2021 classification of central nervous system tumors and implications for therapy for adult-type gliomas: a review. *JAMA Oncol.* 2022;8:1493–501.
8. Cloughesy TF, Cavenee WK, Mischel PS. Glioblastoma: from molecular pathology to targeted treatment. *Annu Rev Pathol.* 2014;9:1–25.
9. De Preter K, Vermeulen J, Brors B, Delattre O, Eggert A, Fischer M, et al. Accurate outcome prediction in neuroblastoma across independent data sets using a multigene signature. *Clin Cancer Res.* 2010;16:1532–41.
10. He W-Q, Gu J-W, Li C-Y, Kuang Y-Q, Kong B, Cheng L, et al. The PPI network and clusters analysis in glioblastoma. *Eur Rev Med Pharmacol Sci.* 2015;19:4784–90.
11. Cheng W, Ren X, Zhang C, Cai J, Liu Y, Han S, et al. Bioinformatic profiling identifies an immune-related risk signature for glioblastoma. *Neurology.* 2016;86:2226–34.
12. Lapointe S, Perry A, Butowski NA. Primary brain tumours in adults. *Lancet (London, England).* 2018;392:432–46.

13. Indraccolo S, Lombardi G, Fassan M, Pasqualini L, Giunco S, Marcato R, et al. Genetic, epigenetic, and immunologic profiling of MMR-deficient relapsed glioblastoma. *Clin Cancer Res.* 2019;25:1828–37.
14. Balana C, Vaz MA, Manuel Sepúlveda J, Mesia C, Del Barco S, Pineda E, et al. A phase II randomized, multicenter, open-label trial of continuing adjuvant temozolomide beyond 6 cycles in patients with glioblastoma (GEINO 14–01). *Neuro Oncol.* 2020;22:1851–61.
15. Voldborg BR, Damstrup L, Spang-Thomsen M, Poulsen HS. Epidermal growth factor receptor (EGFR) and EGFR mutations, function and possible role in clinical trials. *Ann Oncol Off J Eur Soc Med Oncol.* 1997;8:1197–206.
16. Marin B-M, Porath KA, Jain S, Kim M, Conage-Pough JE, Oh J-H, et al. Heterogeneous delivery across the blood-brain barrier limits the efficacy of an EGFR-targeting antibody drug conjugate in glioblastoma. *Neuro Oncol.* 2021;23:2042–53.
17. Neyns B, Sadones J, Joosens E, Bouttens F, Verbeke L, Baurain J-F, et al. Stratified phase II trial of cetuximab in patients with recurrent high-grade glioma. *Ann Oncol Off J Eur Soc Med Oncol.* 2009;20:1596–603.
18. Gan HK, Burgess AW, Clayton AHA, Scott AM. Targeting of a conformationally exposed, tumor-specific epitope of EGFR as a strategy for cancer therapy. *Cancer Res.* 2012;72:2924–30.
19. Langfelder P, Horvath S. WGCNA: an R package for weighted correlation network analysis. *BMC Bioinformatics.* 2008;9:559.
20. Maksimov MO, Pan SJ, James LA. Lasso peptides: structure, function, biosynthesis, and engineering. *Nat Prod Rep.* 2012;29:996–1006.
21. Subramanian A, Tamayo P, Mootha VK, Mukherjee S, Ebert BL, Gillette MA, et al. Gene set enrichment analysis: a knowledge-based approach for interpreting genome-wide expression profiles. *Proc Natl Acad Sci U S A.* 2005;102:15545–50.
22. Gentles AJ, Newman AM, Liu CL, Bratman SV, Feng W, Kim D, et al. The prognostic landscape of genes and infiltrating immune cells across human cancers. *Nat Med.* 2015;21:938–45.
23. Chen R, Smith-Cohn M, Cohen AL, Colman H. Glioma subclassifications and their clinical significance. *Neurother J Am Soc Exp Neurother.* 2017;14:284–97.
24. Zhong Q-Y, Fan E-X, Feng G-Y, Chen Q-Y, Gou X-X, Yue G-J, et al. A gene expression-based study on immune cell subtypes and glioma prognosis. *BMC Cancer.* 2019;19:1116.
25. Louis DN, Perry A, Reifenberger G, von Deimling A, Figarella-Branger D, Cavenee WK, et al. The 2016 World Health Organization Classification of Tumors of the Central Nervous System: a summary. *Acta Neuropathol.* 2016;131:803–20.
26. Louis DN, Perry A, Wesseling P, Brat DJ, Cree IA, Figarella-Branger D, et al. The 2021 WHO Classification of Tumors of the Central Nervous System: a summary. *Neuro Oncol.* 2021;23:1231–51.
27. Wu L, Qu X. Cancer biomarker detection: recent achievements and challenges. *Chem Soc Rev.* 2015;44:2963–97.
28. Yang K, Wu Z, Zhang H, Zhang N, Wu W, Wang Z, et al. Glioma targeted therapy: insight into future of molecular approaches. *Mol Cancer.* 2022;21:39.
29. Dunn GP, Cloughesy TF, Maus MV, Prins RM, Reardon DA, Sonabend AM. Emerging immunotherapies for malignant glioma: from immunogenomics to cell therapy. *Neuro Oncol.* 2020;22:1425–38.
30. Mohammad T, Singh P, Jairajpuri DS, Al-Keridis LA, Alshammari N, Adnan M, et al. Differential gene expression and weighted correlation network dynamics in high-throughput datasets of prostate cancer. *Front Oncol.* 2022;12: 881246.
31. Wang J-S, Wang Y-G, Zhong Y-S, Li X-D, Du S-X, Xie P, et al. Identification of co-expression modules and pathways correlated with osteosarcoma and its metastasis. *World J Surg Oncol.* 2019;17:46.
32. Zhang Z, Chen L, Xu P, Xing L, Hong Y, Chen P. Gene correlation network analysis to identify regulatory factors in sepsis. *J Transl Med.* 2020;18:381.
33. Li Y-M, Li Z-L, Chen F, Liu Q, Peng Y, Chen M. A LASSO-derived risk model for long-term mortality in Chinese patients with acute coronary syndrome. *J Transl Med.* 2020;18:157.
34. Wang W, Liu W. PCLasso: a protein complex-based, group lasso-Cox model for accurate prognosis and risk protein complex discovery. *Brief Bioinform.* 2021;22.
35. Zhang B, Tian J, Dong D, Gu D, Dong Y, Zhang L, et al. Radiomics features of multiparametric MRI as novel prognostic factors in advanced nasopharyngeal carcinoma. *Clin Cancer Res.* 2017;23:4259–69.
36. Qu M, Jiao H, Zhao J, Ren Z-P, Smits A, Kere J, et al. Molecular genetic and epigenetic analysis of NCX2/SLC8A2 at 19q13.3 in human gliomas. *Neuropathol Appl Neurobiol.* 2010;36:198–210.
37. Qu M, Yu J, Liu H, Ren Y, Ma C, Bu X, et al. The candidate tumor suppressor gene SLC8A2 inhibits invasion, angiogenesis and growth of glioblastoma. *Mol Cells.* 2017;40:761–72.
38. Beuschlein F, Boulkroun S, Osswald A, Wieland T, Nielsen HN, Lichtenauer UD, et al. Somatic mutations in ATP1A1 and ATP2B3 lead to aldosterone-producing adenomas and secondary hypertension. *Nat Genet.* 2013;45:440–4.
39. Daniil G, Fernandes-Rosa FL, Chemin J, Blesneac I, Beltrand J, Polak M, et al. CACNA1H mutations are associated with different forms of primary aldosteronism. *EBioMedicine.* 2016;13:225–36.
40. Scholl UI. Genetics of primary aldosteronism. *Hypertens (Dallas, Tex 1979).* 2022;79:887–97.
41. Wang W, Li W, Pan L, Li L, Xu Y, Wang Y, et al. Dynamic regulation genes at microtubule plus ends: a novel class of glioma biomarkers. *Biology (Basel).* 2023;12:488.
42. Grasso S, Cangelosi D, Chapelle J, Alzona M, Centonze G, Lamolinara A, et al. The SRCIN1/p140Cap adaptor protein negatively regulates the aggressiveness of neuroblastoma. *Cell Death Differ.* 2020;27:790–807.
43. Heimberger AB, Abou-Ghazal M, Reina-Ortiz C, Yang DS, Sun W, Qiao W, et al. Incidence and prognostic impact of FoxP3+ regulatory T cells in human gliomas. *Clin Cancer Res.* 2008;14:5166–72.
44. Gieryng A, Pszczolkowska D, Walentynowicz KA, Rajan WD, Kaminska B. Immune microenvironment of gliomas. *Lab Investig.* 2017;97:498–518.
45. Nduom EK, Weller M, Heimberger AB. Immunosuppressive mechanisms in glioblastoma. *Neuro Oncol.* 2015;17(Suppl 7):vii9–14.
46. Mangani D, Weller M, Roth P. The network of immunosuppressive pathways in glioblastoma. *Biochem Pharmacol.* 2017;130:1–9.